

# Correlation between Mitochondria-Associated Endoplasmic Reticulum Membrane-Related Genes and Cellular Senescence-Related Genes in Osteoarthritis

Hui-Min Li,<sup>†</sup> Chenhuan Wang,<sup>†</sup> Qixue Liu, Zhicheng Tong, Binghua Song, Wei Wei,<sup>\*</sup> and Chong Teng<sup>\*</sup>



Cite This: *ACS Omega* 2024, 9, 19169–19181



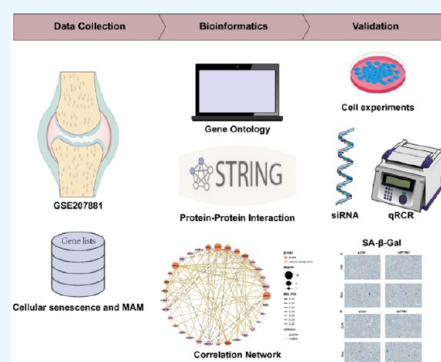
Read Online

ACCESS |

Metrics & More

Article Recommendations

**ABSTRACT:** Background: The role of mitochondria-associated endoplasmic reticulum membrane (MAM) formation in the development of osteoarthritis (OA) is yet unclear. Methods: A mix of bioinformatics methods and *in vitro* experimental methodologies was used to study and corroborate the role of MAM-related genes and cellular senescence-related genes in the development of OA. The Gene Expression Omnibus database was used to obtain the microarray information that is relevant to the OA. Several bioinformatic methods were employed to carry out function enrichment analysis and protein–protein correlation analysis, build the correlation regulatory network, and investigate potential relationships between MAM-related genes and cellular senescence-related genes in OA. These methods also served to identify the MAM-related and OA-related genes (MAM-OARGs). Results: For the additional functional enrichment analysis, a total of 13 MAM-OARGs were detected. The correlation regulatory network was also created. Hub MAM-OARGs were shown to have a strong correlation with genes relevant to cellular senescence in OA. Results of *in vitro* experiments further demonstrated a positive correlation between MAM-OARGs (PTPN1 and ITPR1) and cellular senescence-related and OA-related genes. Conclusions: As a result, our findings can offer new insights into the investigations of MAM-related genes and cellular senescence-related genes, which could be linked to the OA as well as brand-new potential treatment targets.



## INTRODUCTION

The most prevalent kind of arthritis, osteoarthritis (OA), is defined by the pathological development of osteophytes and inflammation of the synovium as well as the gradual loss of cartilage matrix. By 2030, it is anticipated that more than 67 million individuals would have OA, with yearly treatment expenses reaching \$3 billion. Therefore, OA is a huge financial and health burden.<sup>1–6</sup> The current standard of therapy for OA involves pain relief and eventually total joint replacement; the former just addresses symptoms and improves joint function, but the latter is linked to infection and other comorbidities. The development of OA cannot be prevented or suppressed, however, because of the lack of efficient disease-modifying therapies.<sup>7</sup>

In general, aging and abnormal mechanical stress-induced alterations in the chondrocyte microenvironment are linked to the etiology of OA.<sup>8–12</sup> Given that OA chondrocytes display a range of senescence-related characteristics, it is believed that chondrocyte senescence may significantly contribute to the pathophysiology of OA. Through metalloproteinase components of the senescence-associated secretory phenotype (SASP) response, chondrocyte senescence is predicted to cause a change in the balance from the creation to breakdown of extracellular

matrix, accelerating the course of the disease.<sup>13</sup> The molecular processes governing the control of cellular senescence in OA are not yet unknown.

Recently, some researchers demonstrated that the increased mitochondria-associated endoplasmic reticulum membrane (MAM) formation is sufficient to trigger premature cellular senescence, involving a mitochondrial ROS/p53 pathway and a partial NFκB-dependent SASP induction.<sup>14</sup> The outer mitochondrial membrane (OMM) in the dynamic network of mitochondria through a special structure known as the MAM, communicates with the endoplasmic reticulum membrane.<sup>15–19</sup> Besides, MAM dynamic formation regulates mitochondrial dynamics, autophagy, inflammation, and apoptosis in addition to being implicated in lipid metabolism, calcium signaling, and redox signaling.<sup>20</sup> Therefore, this study was designed to explore

Received: December 24, 2023

Revised: March 21, 2024

Accepted: April 1, 2024

Published: April 15, 2024



Table 1. Primers Used for qPCR

gene	primers sequence (5'-3')	
	forward	reverse
ACTB	CAGATGTGGATCAGCAAGCAGGAG	CGCAACTAAGTCATAGTCCGCCTAG
GSK3B	GTGTTGGCTGAGCTGTTACTAGGAC	CAGTGGTGTAGTCGGGCAGTTG
ITPR1	CACTCGCAGCAAGACTACAGGAAG	AGACACAGAGGTCGGAGAGTAATC
PTPN1	GCTGATACCTGCCTCTTGTCTGATG	ATCCTCCTGGGTCTCTTCCTTCAAC
CDKN1A	GATGGAACCTTCGACTTTGTTCAC	GTCCACATGGTCTTCTCTCTG
CDKN2A	GGCACCAGAGGCAGTAACCATG	AGTTGTGGCCCTGTAGGACCTTC
MAP2K1	CAAGCCCTCCAACATCCTAGTCAAC	ATACCTCCCAACCGCCATCTCTAC
MAPK14	CTGGCTCGGCACACAGATGATG	GGGTGTTCTGTGAGACGCATAATC
PTEN	TGGAAGGGACGAACTGGTGTAAATG	CGTCGTGTGGGTCTGAAATGG
TWIST1	GGAGTCCGCAGTCTTACGAGGAG	GTCGCTCTGGAGGACCTGGTAG
ABL1	GCTTCTTGGTGCCTGAGAGTGAG	CTGGATAATGGAGCGTGGTGTATGAG

the relationship between MAM-related genes and cellular senescence-related genes in OA.

We have established the following items in this work by using a variety of established bioinformatic methodologies and *in vitro* experimental techniques: (1) the dysregulated MAM-related genes of OA, their primary biological functions, and likely hub MAM-related genes; (2) the potential association between MAMRGs and cellular senescence-related genes in senescence chondrocyte and OA.

## MATERIALS AND METHODS

**Data Collection and Processing.** Information on the gene expression of mRNA was downloaded from the Gene Expression Omnibus (GEO) database, which may be found at <https://www.ncbi.nlm.nih.gov/geo/>. The data set for this study was chosen based on the following criteria: Patients had to meet the American College of Rheumatology's definition of OA and not have a history of knee injuries, operations, rheumatoid arthritis, or pseudogout. Their knee joint X-ray pictures showed OA, which was validated. *Homo sapiens* is the species, cartilage in both healthy cartilage tissues and OA cartilage tissues is the sample, and microarray or next-generation sequencing data is the sequencing technique. This study excluded the following data sets: expression data from other tissues, surgically removed cartilage tissues, individuals with rheumatoid arthritis, and cartilage tissues from knee injuries (such as blood samples). The GSE207881 mRNA expression data set was ultimately selected and downloaded for further analysis. This data set's expression files were compiled using microarray data from 59 OA cartilage tissues and 6 healthy cartilage tissues. CSRGs were retrieved from the Molecular Signatures database's Gene Set GOBP CELLULAR SENESCENCE (<http://www.gsea-msigdb.org/gsea/msigdb/index.jsp>). A total of 68 MAM genes were included in the MAM-related genes, which were gathered from earlier research.<sup>21</sup>

**Identification of MAM-Related and OA-Related Genes (MAM-OARGs).** The R/Bioconductor affy program was used to standardize the raw data. OA-related genes were identified using the R package limma, with the criterion of  $p < 0.05$  and fold change  $> 1.5$ .<sup>22,23</sup> By using a Venn diagram to link the OA-related genes with MAMRGs, we found the MAM-OARGs were found.

**Gene Ontology Functional Analysis.** To comprehend the biological process, cellular components, and molecular function of MAM-OARGs, Gene Ontology (GO) research was conducted. Wiki pathway analysis was used to look at the MAM-OARGs' related signaling pathways. The Enrichr database was used to conduct the GO and Wiki pathway analyses,

and particular results of the GO and Wiki pathway analyses with  $p < 0.05$  were selected for further visualization.<sup>24</sup>

**Protein–Protein Interaction (PPI) Analysis of MAM-OARGs.** The STRING database (<https://cn.string-db.org/>) was a widely used tool to explore the association networks of functional proteins.<sup>25</sup> PPI analysis was conducted using the STRING database by imputing the MAM-OARGs into the multiple protein section, and protein pairs with a score  $> 0.40$  were selected to construct the PPI network by Cytoscape software (<https://cytoscape.org/>). The PPI score was calculated using the Degree method by the cytoHubba plug-in, and all MAM-OARGs ranked by the PPI score were selected for further analysis.

**Correlation Analysis Among MAM-OARGs.** The Spearman test was used to conduct a correlation study across MAM-OARGs to investigate any possible relationships between them in OA. Correlated pairs with  $|r| > 0.20$  and  $p < 0.05$  was considered statistically significant. Additionally, a correlation network based on couples with  $|r| > 0.20$  and  $p < 0.05$  was constructed.

**Identification of Cellular Senescence-Related and OA-Related Genes (CS-OARGs).** Genes associated with cellular senescence and OA were intersected using a Venn diagram to get the associated genes for cellular senescence and OA. The analysis of CS-OARGs was then done using GO and Wiki pathways. The top 20 hub CS-OARGs were then determined utilizing the degree approach and PPI analysis of CS-OARGs using Cytoscape software. In order to investigate possible connections between hub CS-OARGs in OA, the Spearman test was used to correlate them. A correlation network was created by Cytoscape software based on couples with  $|r| > 0.20$  and  $p < 0.05$ .

**Correlation Analysis Between MAM and Cellular Senescence.** The PPI analysis of hub CS-OARGs and MAM-OARGs was conducted. Next, the correlation analysis between hub CS-OARGs and MAM-OARGs was carried out using the Spearman test to investigate any possible relationships between MAM and cellular senescence in OA, and the regulatory network was built by integrating the pairs with  $|r| > 0.20$  and  $p < 0.05$ .

**In Vitro Experimental Verification. Cell Culture.** The laboratory of Professor Mary B. Goldring (Hospital for Special Surgery/Weill Medical College of Cornell University, New York, NY) developed the immortalized human chondrocyte cell line C28/I2, which was isolated from the costal cartilage of a 15-year-old female and immortalized using SV-40 large T-antigen.<sup>26</sup> 10% FBS (10%) was added to DMEM/high-glucose media, which was used to cultivate C28/I2 cells. When the cells had

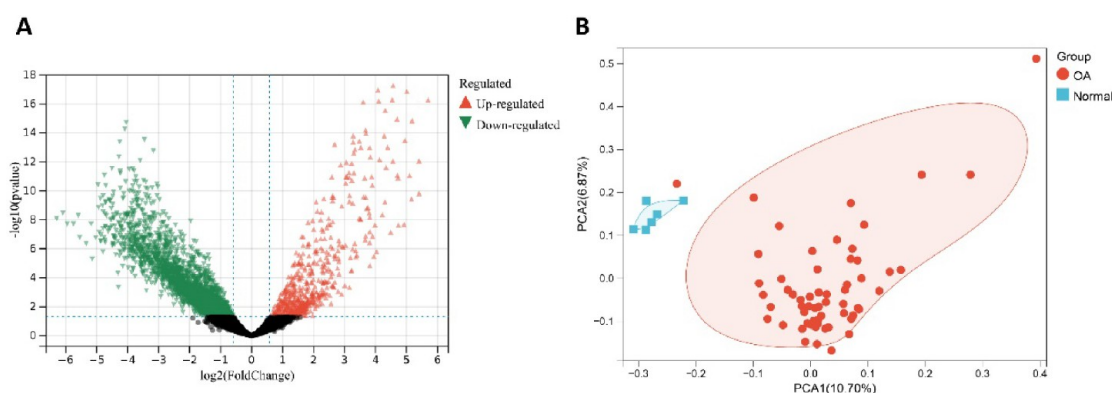


**Figure 1.** (A) Volcano plot of the OA-related genes. (B) PCA of OA and normal samples. The black dots represent RNAs that are not differentially expressed, and the red and green dots represent the upregulated and downregulated RNAs, respectively.

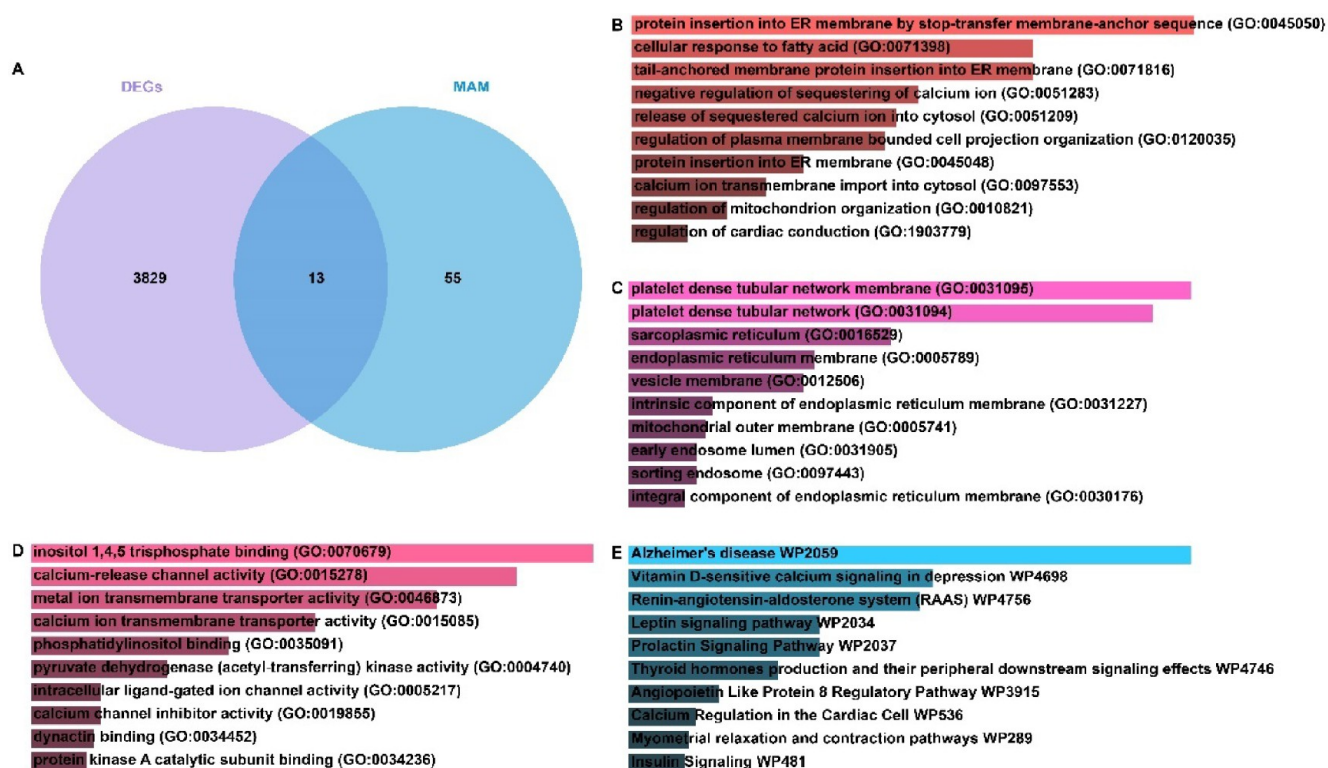


**Figure 2.** (A) Intersection between MAMGRs and OA-related genes. GO (biological process, cell component, and molecular function) and KEGG annotation for the MAM-OARGs: (B) biological process; (C) cell component; (D) molecular function; (E) pathway. Ranking by  $-\log_{10}(p\text{-value})$ . MAM, mitochondria-associated endoplasmic reticulum membrane; MAMGRs, MAM-related genes; MAM-OARGs, MAM-related and OA-related genes.

reached around 90% confluence, they were separated using a trypsin-EDTA (Gibco) solution and split in fresh media. C28/I2 cells were exposed to 100 ng/mL doxorubicin (SC0159, Beyotime, China) for 7 days in order to cause senescence in the cells. Every 2 days, the doxorubicin-containing medium was changed.

**Transfection and Treatment.** The PTPN1 or ITPR1 siRNA (GenePharma, Shanghai, China) or the negative control siRNA were transfected into chondrocytes for a duration of 48 h using the Lipofectamine RNAiMAX Reagent from Invitrogen, California. For an extra 24 h following transfection, chondrocytes were exposed to 100 ng/mL dox (SC0159, Beyotime, China) in an attempt to replicate the cellular senescence milieu associated with osteoarthritis.

**Quantitative Real-Time PCR.** Utilizing the TRIzol reagent (Invitrogen), total RNA was isolated from cells according to the manufacturer's instructions. HiScript QRT SuperMix produced the cDNA (Vazyme, Nanjing, China). qPCR was carried out using the ABI Step-One Plus™ Real-Time PCR System and ChamQ SYBR qPCR Master Mix (Vazyme) (Applied Biosystems). The data were analyzed following the  $2^{-\Delta\Delta Ct}$  method, and *ACTB* was used as an internal check to normalize the results. All primers are listed in Table 1.

**SA- $\beta$ -Gal Staining.** Using a cell senescence  $\beta$ -galactosidase staining kit from Beyotime Biotechnology and following the manufacturer's instructions, SA- $\beta$ -Gal staining was performed. Briefly, cells were rinsed with PBS before being fixed in 2% PFA and 0.2% glutaraldehyde for 5 min. The cells were then cleaned

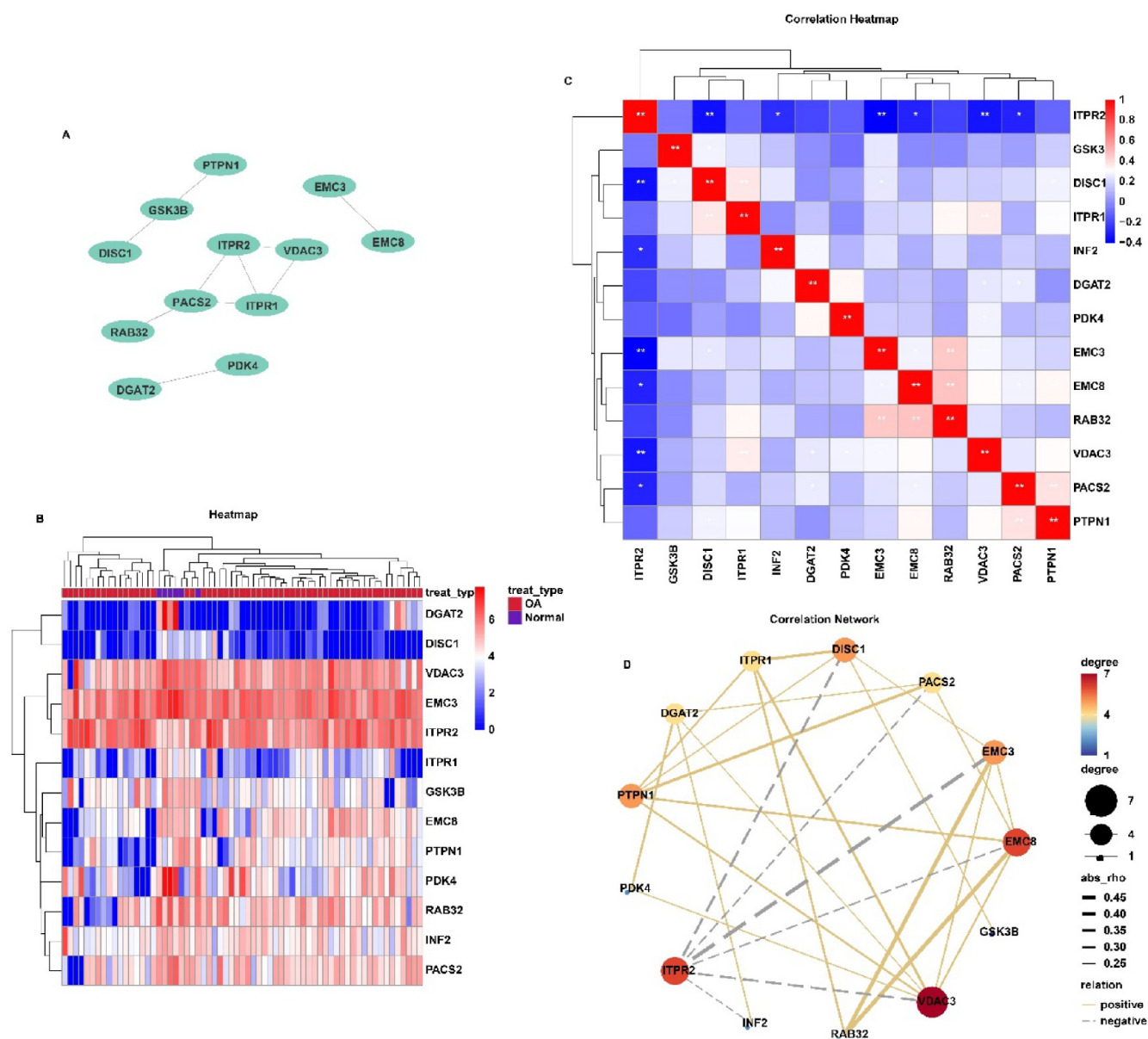


**Figure 3.** (A) PPI network of MAM-OARGs; (B) heat map of expression of MAM-OARGs; (C) eat map of correlation of MAM-OARGs; (D) correlation network of MAM-OARGs. MAM, mitochondria-associated endoplasmic reticulum membrane; MAM-OARGs, MAM-related and OA-related genes.

and allowed to sit in the SA- $\beta$ -Gal staining solution at 37 °C for 16 h. The cells were rinsed after incubation, and an Eclipse Ni-U 131 microscope was used to photograph them (Nikon). Using ImageJ, the number of total cells and SA- $\beta$ -Gal-positive cells were determined in three random areas per culture dish.

**Statistical Analysis.** Results are presented as mean  $\pm$  SEM. Statistical significances were calculated with Student's *t* test for comparisons between 2 groups and ANOVA for multiple-group comparisons as shown in figure legends. *p* values were considered significant at \**p* < 0.05, \*\**p* < 0.01, and \*\*\**p* < 0.001.

## RESULTS

**Determination of OA-Related Genes and MAM-OARGs.** As shown in the volcano plot (Figure 1A), a total of 3842 OA-related genes were identified with the criterion of fold change >1.5 and *p* < 0.05. Principal component analysis (PCA)

revealed that OA cartilage tissues and normal cartilage tissues could be distinguished from one another clearly using cluster analysis (Figure 1B). By combination of MAMRGs with OA-related genes, a total of 13 MAM-OARGs were created (Figure 2A).

**GO and KEGG Enrichment Analysis of MAM-OARGs.** The GO analysis, which consisted of biological processes, cell components, and molecular functions, was conducted to explore the biological functions of MAM-OARGs. The biological process of these MAM-OARGs was mainly enriched at the protein insertion into ER membrane by stop-transfer membrane-anchor sequence, cellular response to fatty acid, tail-anchored membrane protein insertion into ER membrane, negative regulation of sequestering of calcium ion, and release of sequestered calcium ion into cytosol (Figure 2B). These MAM-OARGs elicited the cell component mainly at the platelet dense tubular network membrane, sarcoplasmic reticulum, endoplas-

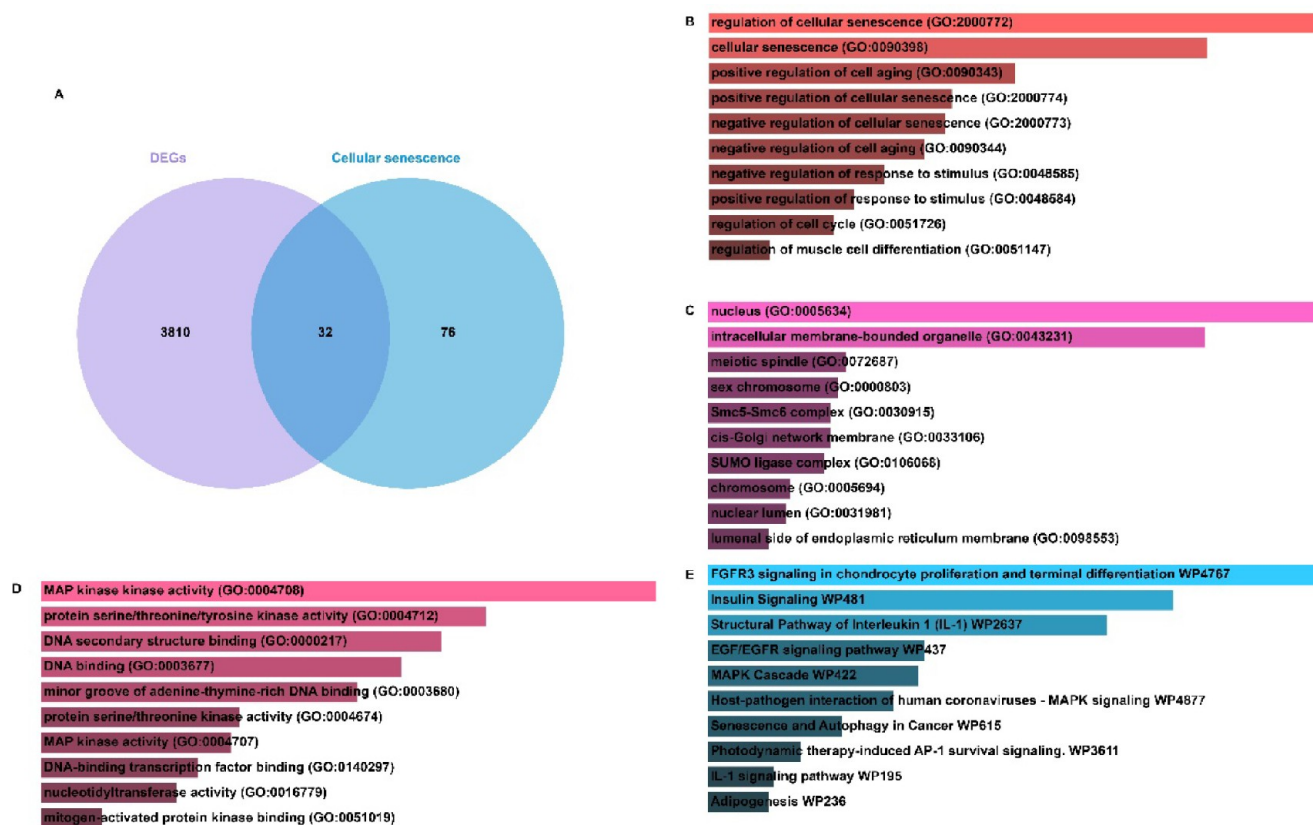


**Figure 4.** (A) Intersection between CS-related genes and OA-related genes (CS-OARGs). GO (biological process, cell component, and molecular function) and KEGG annotation for the CS-OARGs: (B) biological process; (C) cell component; (D) molecular function; and (E) pathway. Ranking by  $-\log_{10}(p\text{-value})$ . CS-OARGs, cell-senescence-related and OA-related genes.

mic reticulum membrane, and mitochondrial outer membrane (Figure 2C), and the most common molecular function of these MAM-OARGs was the inositol 1,4,5 trisphosphate binding, calcium-release channel activity, and pyruvate dehydrogenase (acetyl-transferring) kinase activity (Figure 2D). Wiki pathway analysis showed these MAM-OARGs were mainly involved in the following biological pathways: Vitamin D-sensitive calcium signaling in depression, the leptin signaling pathway, and calcium regulation in the cardiac cell (Figure 2E).

**PPI Analysis and Correlation Analysis Among MAM-OARGs.** PPI analysis of 13 MAM-OARGs was conducted with a network of 13 nodes and 10 edges (PPI enrichment  $p < 0.01$ ) (Figure 3A). The heat map showed the expression of these MAM-OARGs between normal cartilage tissues and OA cartilage tissues (Figure 3B). The correlation analysis among MAM-OARGs was conducted (Figure 3C); EMC8-RAB32 pair was the most positively correlated pair ( $r = 0.47, p < 0.01$ ), and EMC3-ITPR2 pair was the most negatively correlated pair ( $r = -0.45, p < 0.01$ ) (Figure 3D).

**Determination of CS-OARGs.** A total of 32 CS-OARGs were obtained by the intersection of CSRGs and OA-related genes (Figure 4A). The biological process of these CS-OARGs was mainly enriched with the regulation of cellular senescence, positive regulation of cell aging, negative regulation of cellular senescence, and regulation of the cell cycle (Figure 4B). These CS-OARGs elicited the cell component mainly at the nucleus, intracellular membrane-bound organelle, and nuclear lumen (Figure 4C), and the most common molecular function of these CS-OARGs was the MAP kinase kinase activity, DNA secondary structure binding, and DNA-binding transcription factor

binding (Figure 4D). Wiki pathway analysis showed these CS-OARGs were mainly involved in the following biological pathways: FGFR3 signaling in chondrocyte proliferation and terminal differentiation, insulin signaling, and the MAPK cascade (Figure 4E).

**PPI Analysis and Correlation Analysis Among CS-OARGs.** PPI analysis of 32 CS-OARGs was conducted with a network of 32 nodes and 39 edges (PPI enrichment  $p < 0.01$ ) (Figure 5A). A total of 20 hub CS-OARGs were selected (Figure 5B), and the heat map showed the expression of these hub CS-OARGs between the normal cartilage tissues and OA cartilage tissues (Figure 5C). The correlation analysis among hub CS-OARGs was conducted (Figure 5D); HMGA1–HMGA2 pair was the most positively correlated pair ( $r = 0.64, p < 0.01$ ), and HMGA2–MAP2K6 pair was the most negatively correlated pair ( $r = -0.57, p < 0.01$ ) (Figure 5E).

**PPI Analysis and Correlation Analysis Between MAM-OARGs and CS-OARGs.** PPI analysis of MAM-OARGs and CS-OARGs was conducted with a network of 32 nodes and 58 edges (PPI enrichment  $p < 0.01$ ) (Figure 6A). The correlation analysis between MAM-OARGs and CS-OARGs was conducted, and the correlation network was also constructed (Figure 6B,C). PPI analysis and correlation analysis are combined; MAM-OARGs, including GSK3B, PTPN1, and ITPR1, might be more related to CS-OARGs, including PTEN, ABL1, MAPK14, and MAP2K1.

**In Vitro Experimental Verification. Inducing Cellular Senescence of Chondrocytes.** To determine the expression of MAM-OARGs and CS-OARGs, we first induced cellular senescence of chondrocytes using doxorubicin for 7 days. We

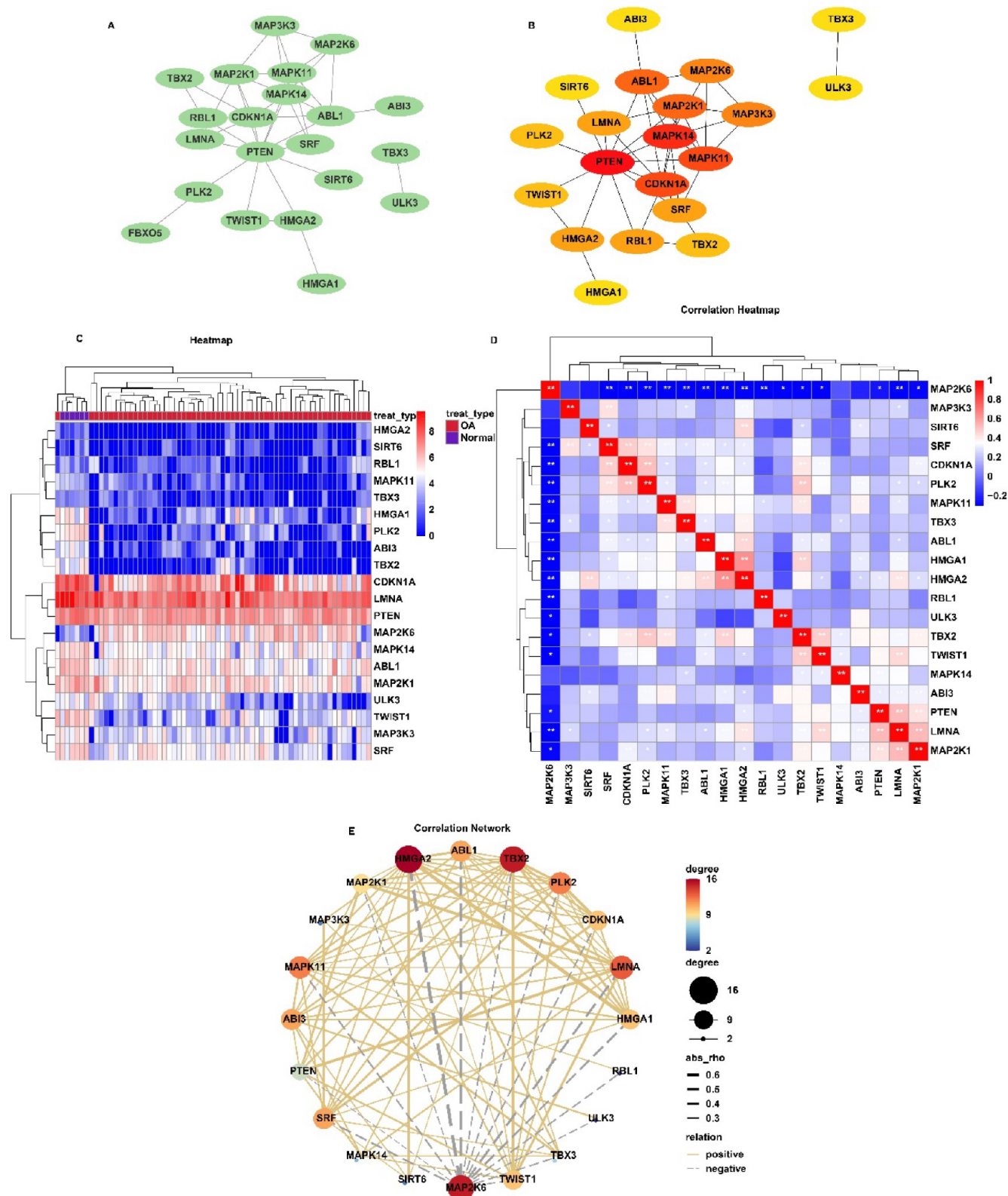


**Figure 5.** (A) PPI network of CS-OARGs; (B) PPI network of 20 hub CS-OARGs; (C) heat map of expression of CS-OARGs; (D) heat map of correlation of CS-OARGs; (E) correlation network of CS-OARGs. CS-OARGs, cellular senescence-related and OA-related genes.

observed the accumulation and phenotypical characterization of senescent chondrocytes in doxorubicin group, including increased expression levels of senescence-associated  $\beta$ -galactosidase (SA- $\beta$ -Gal), CDKN1A, and CDKN2A, according to SA- $\beta$ -gal staining and qPCR (Figure 7A,B).

**Expression of MAM-OARGs and CS-OARGs.** Compared with the control group, the MAM-OARGs, including PTPN1 and ITPR1, were significantly upregulated in the senescent chondrocytes. However, there was no statistical difference in the expression of GSK3B in either group (Figure 7C). Besides,

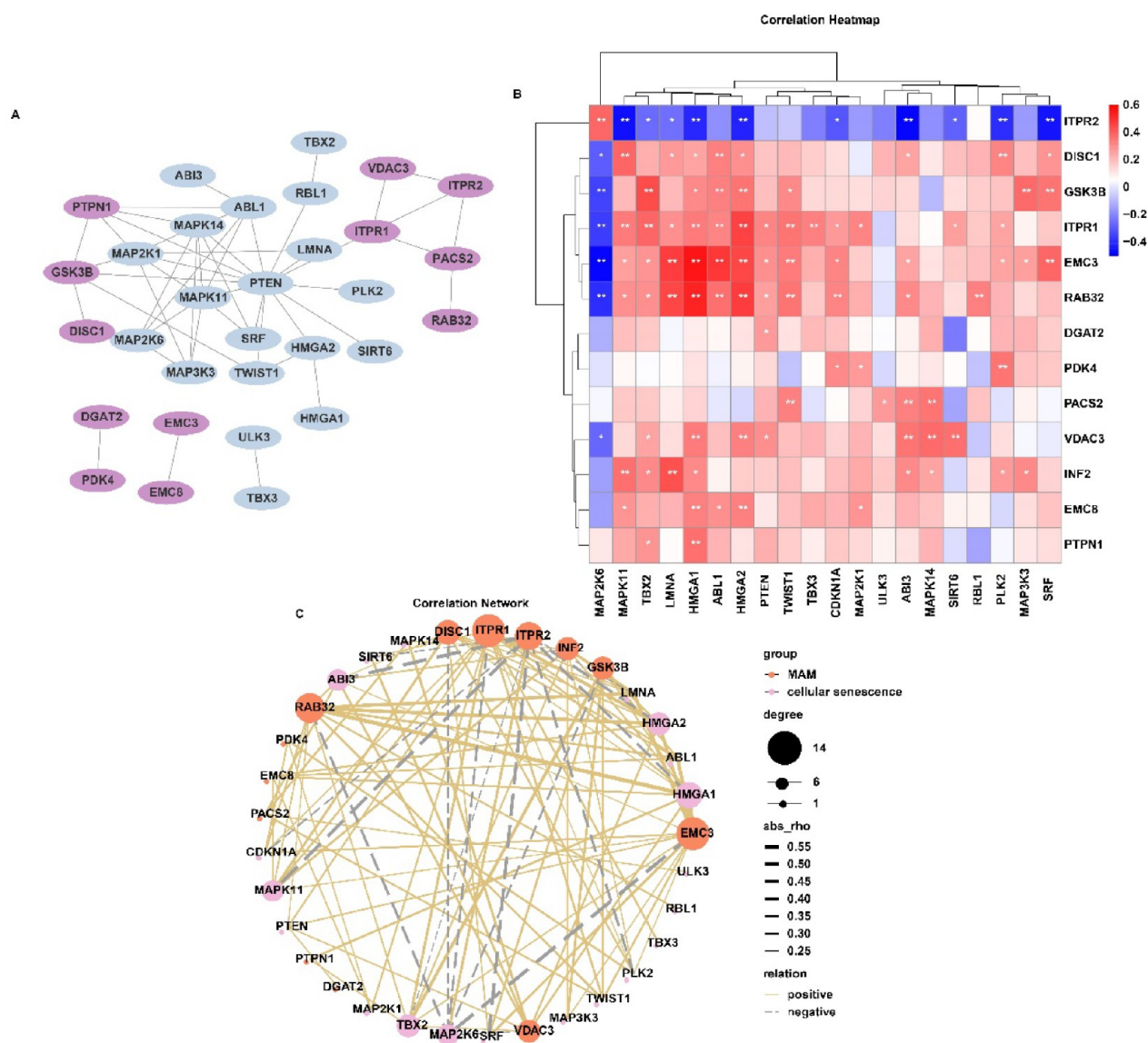


**Figure 6.** (A) PPI network of MAM-OARGs and CS-OARGs; (B) heat map of correlation of MAM-OARGs and CS-OARGs; (C) correlation network of MAM-OARGs and CS-OARGs. MAM, mitochondria-associated endoplasmic reticulum membrane; CS-OARGs, cellular senescence-related and OA-related genes. MAM-OARGs, MAM-related and OA-related genes.

the CS-OARGs, including PTEN, ABL1, MAPK14, and MAP2K1, were significantly upregulated in the senescent chondrocytes compared with the control group (Figure 7D). Additionally, the findings of the correlation analysis demonstrated a positive association between MAM-OARGs, including PTPN1 and ITPR1, and CS-OARGs, including PTEN, ABL1, MAPK14, and MAP2K1 (Figure 8A,B).

**Effects of MAM-OARGs Knockdown on Chondrocyte Senescence.** We demonstrated that PTP1B and ITPR1 control senescence by inhibiting chondrocyte senescence with PTPN1siRNA or ITPR1siRNA. By blocking PTP1B and ITPR1, we also observed a decrease in the morphological features and accumulation of senescent chondrocytes, as demonstrated by SA- $\beta$ -Gal staining (Figure 9A,B). ABL1, MAPK14, and MAP2K1 are among the CS-OARGs whose expression may be inhibited by PTP1B and ITPR1 knockdown (Figure 9C,D).

## DISCUSSION

In this study, we used a range of bioinformatic approaches to filter out 13 MAM-OARGs, describe their relevant GO biological functions, and create correlation networks. We also proposed a relationship between MAM-related genes and cellular senescence-related genes in OA. Finally, *in vitro* experimental confirmation suggests that MAM-OARGs (PTPN1 and ITPR1) were positively correlated with CS-OARGs (PTEN, ABL1, MAPK14, and MAP2K1). Our results contributed to the body of information about the correlation of MAM-related genes and cellular senescence-related genes in OA.

Evidence suggesting a modification of their contacts and quality with various age-related disorders or aging have recently proposed a function for MAM formation in aging.<sup>27–29</sup> In Alzheimer's disease patients, MAM formation are increased and three enzymes (presenilin-1, presenilin-2, and  $\gamma$ -secretase) that contribute to the production of amyloid  $\beta$  colocalize at MAM.<sup>30</sup> The majority of Parkinson disease-related proteins, including  $\alpha$ -

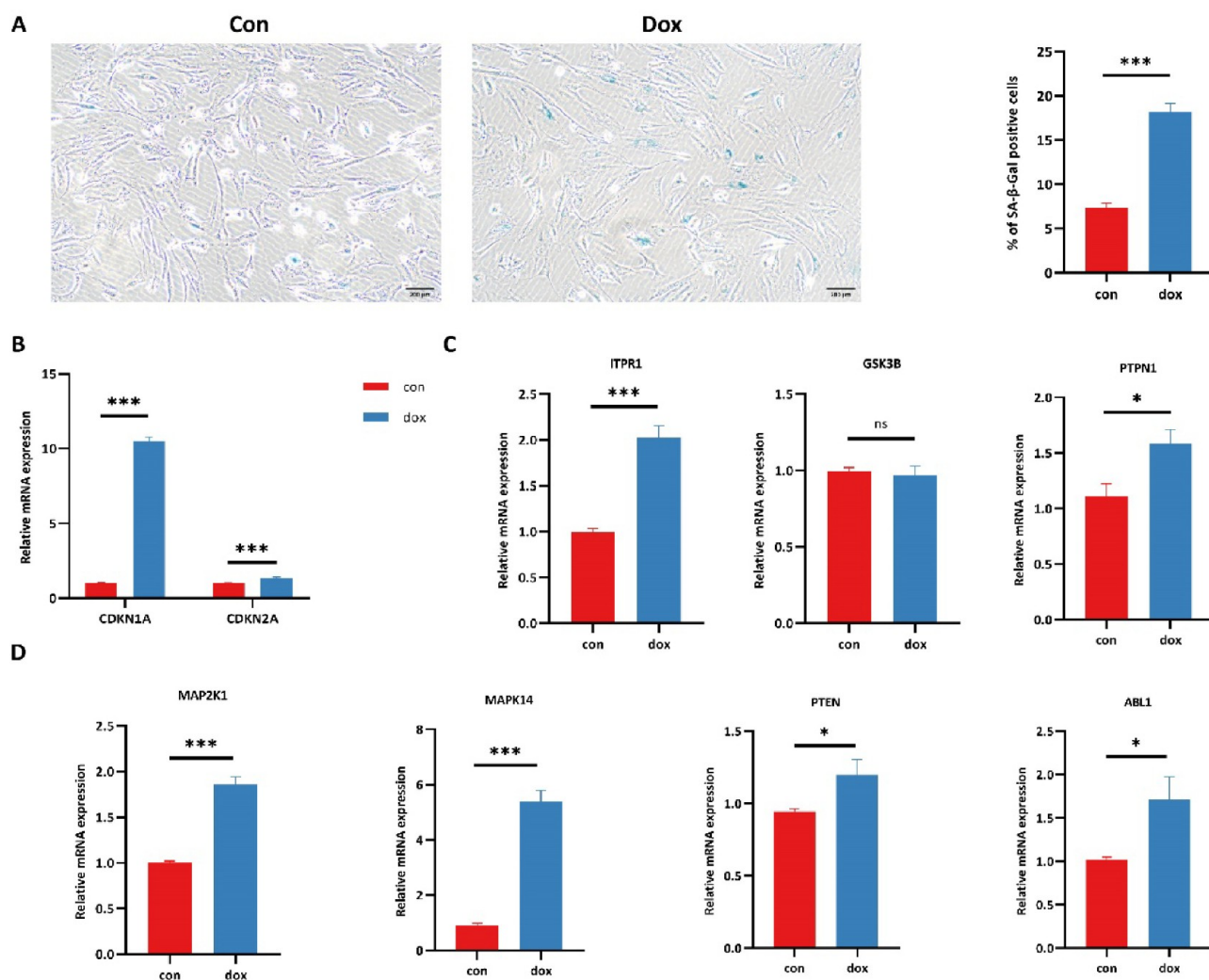


**Figure 7.** (A) Representative images of SA- $\beta$ -Gal staining C28/I2 cells were derived from the control group and doxorubicin (dox) group and subsequent quantification of SA- $\beta$ -Gal staining C28/I2 cells.  $n = 3$ , \*\*\* $p < 0.001$ . (B) QPCR analysis of mRNA levels of CDKN1A and CDKN2A in C28/I2 cells derived from control group and doxorubicin (dox) group,  $n = 6$ , \*\*\* $p < 0.001$ . (C) QPCR analysis of mRNA levels of MAM-OARGs, including PTPN1, GSK3B, and ITPR1, in C28/I2 cells derived from control group and doxorubicin (dox) group,  $n = 6$ , ns  $p > 0.05$ , \* $p < 0.05$ , \*\*\* $p < 0.001$ . (D) QPCR analysis of mRNA levels of CS-OARGs, including MAP2K1, MAPK14, PTEN, and ABL1, in C28/I2 cells derived from control group and doxorubicin (dox) group,  $n = 6$ , \* $p < 0.05$ , \*\*\* $p < 0.001$ . All data were presented as mean  $\pm$  SEM. Student's  $t$  test was used for statistical analysis.

synuclein, Parkin, or PINK1, are located in the MAM fraction, and MAM structure is changed in patients with Parkinson's disease. In addition, it has been proposed that Mfn2 deletion influences MAM amount, albeit its exact function is yet unknown. In a mouse model, it also causes nonalcoholic steatohepatitis, one of the most severe phases of nonalcoholic fatty liver disease (NAFLD).<sup>31</sup> More recently, it was determined how the ER-mitochondrial calcium flow affects aging in worms and mice. One side of the issue is that ablation of the mouse ER-calcium release channel ITPR2 lengthens longevity exclusively in females and decreases MAM and age-related changes in both males and females.<sup>14</sup> However, in worms, ATF-6 loss of function leads to long-lasting ITPR-mediated ER-mitochondria fluxes that increase life span.<sup>32</sup> All things considered, these investigations show that MAM and cellular senescence have various correlations in controlling aging and can control comparable age-related diseases. Nevertheless, the number of research studies examining MAMs' role in OA is still rather few. In this work, we first identified the pertinent GO biological

functions of 13 MAM-OARGs by filtering them out using a variety of bioinformatic techniques. Additionally, MAM formation and mitochondrial calcium uptake are also improved by  $\alpha$ -synuclein.<sup>33,34</sup> The major organelles that control intracellular calcium ( $\text{Ca}^{2+}$ ) homeostasis are the ER and mitochondria, and it is well known that  $\text{Ca}^{2+}$  is transported from the ER lumen into the mitochondria by MAMs, which is crucial for many different aspects of cellular function. By activating the rate-limiting enzymes of the TCA cycles and ATP synthase, for example, temporary mitochondrial  $\text{Ca}^{2+}$  intake via MAMs increases mitochondrial oxidative respiration and ATP production.<sup>35,36</sup> In fact, the Wiki pathway analysis of our data revealed that MAM-OARGs were primarily involved in controlling calcium ion sequestration. Multiple calcium channels, including ITPRs (ITPR1, 2, and 3), VDACs (1, 2, and 3), MCU at the IMM for the mitochondrial influx, and SERCA (1, 2) for the ER influx, control calcium exchanges at the MERCs interface. In our study, ITPR1 was discovered to be elevated by bioinformatic techniques and gene expression



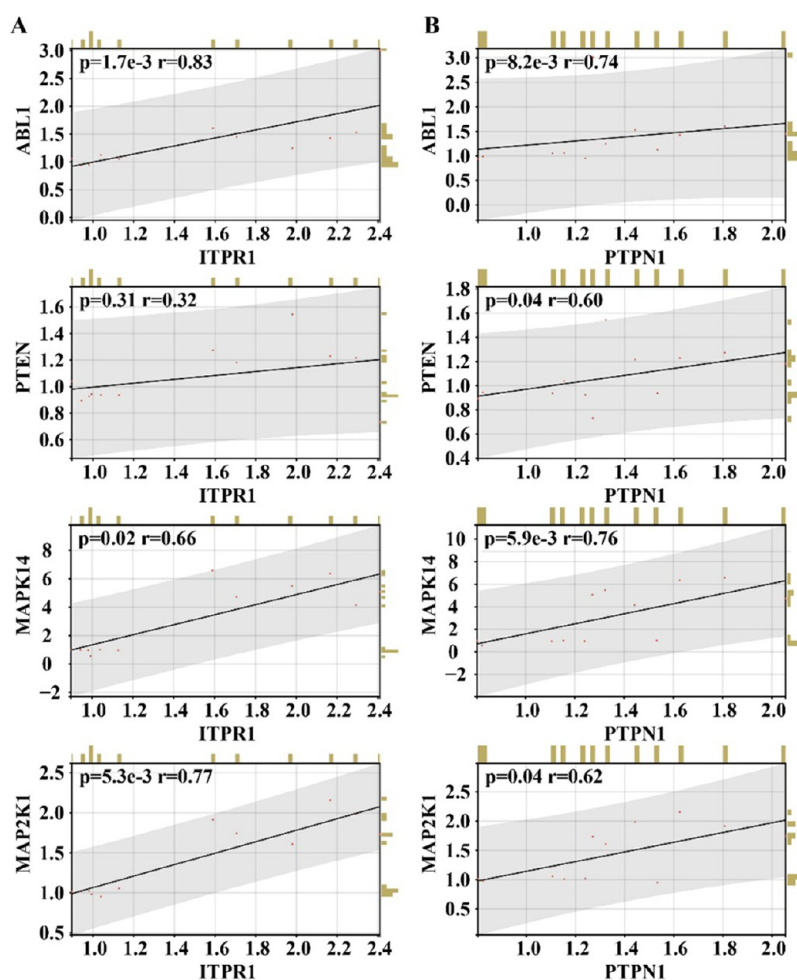


**Figure 8.** (A) Correlation analysis of ITPR1 with CS-OARGs, including MAP2K1, MAPK14, PTEN, and ABL1. (B) Correlation analysis of PTPN1 with CS-OARGs, including MAP2K1, MAPK14, PTEN, and ABL1.

analysis *in vitro* experiments. A few research examined the role of ITPRs in functionally controlling cellular senescence at the ER interface. Human mammary epithelial cells (hMECs) that have had ITPR2 knocked down are able to resist oncogene-induced senescence (OIS), but normal human fibroblasts also experience a delay in replicative senescence.<sup>37</sup> Further research revealed that forced interactions between the mitochondria and the ER cause premature senescence<sup>14</sup> and that ITPR2 ablation reduced the frequency of contacts between the mitochondria and the ER in both *in vivo* and *in vitro* experiments. Additionally, deactivating ITPR1 and ITPR3 was similarly effective in delaying senescence.<sup>37</sup> It is yet to be determined if ITPR1 plays a part in the onset of OA, and whether this activity is MAM-dependent. Similarly, we discovered that in the dox-inducing cellular senescence group, the expression of PTPN1 (encoding PTP1B) was increased. The widely varying cellular signaling networks are significantly regulated by the classical protein tyrosine phosphatase PTP1B. For a very long time, it was believed that PTP1B only had an impact when it was perched in the ER. In prior work, it was discovered that the inactivation of PTP1B was both essential and sufficient to cause premature senescence in IMR90 fibroblasts that expressed H-RAS(V12).<sup>38</sup> When SirT1 was expressed in chondrocytes, IGFR, phosphatidylinositol 3-kinase, phosphoinositide-dependent protein kinase 1, mTOR, and Akt were all activated. These kinases, in turn, phosphorylated MDM2, inhibited p53, and prevented apoptosis. At least in part,

PTP1B is suppressed by SirT1 to activate the IGFR.<sup>39</sup> PTPIP51 (protein tyrosine phosphatase interacting protein 51) was shown to be connected to the insulin signaling pathway via PTP1B and 14-3-3beta in other studies.<sup>40</sup> In a neuroblastoma cell line that resembles motor neurons, overexpression of PTPIP51 (OMM) and VAPB (ER) significantly increased the ER-mito contacts.<sup>41</sup> However, in order to fully understand this putative function of PTP1B in the synthesis of MAM and its function in controlling cellular senescence, more detailed studies need to be carried out in the future.

According to several research, the number of senescent chondrocytes and synovial fibroblasts substantially corresponds with aging, and joint tissues, like other organs, are vulnerable to senescence and deterioration with time.<sup>42,43</sup> Senescent joint cells share characteristics such as telomere thinning, increased expression of p53, p21, and p16, increased ROS production due to mitochondrial failure, and increased heterochromatin that is linked with senescence.<sup>44</sup> In recent work, Zhu et al.<sup>45</sup> described the use of microRNA (miRNA) to target cellular senescence in order to repair the articular microenvironment, offering OA patients a potentially effective treatment option. The substantial relationship found in our study points to a potential connection between MAM-related genes and cellular senescence-related genes in OA. We initially identified 20 hub CS-OARGs using the correlation network analysis, and then we utilized the Spearman analysis to try to understand how they link to MAM-OARGs.

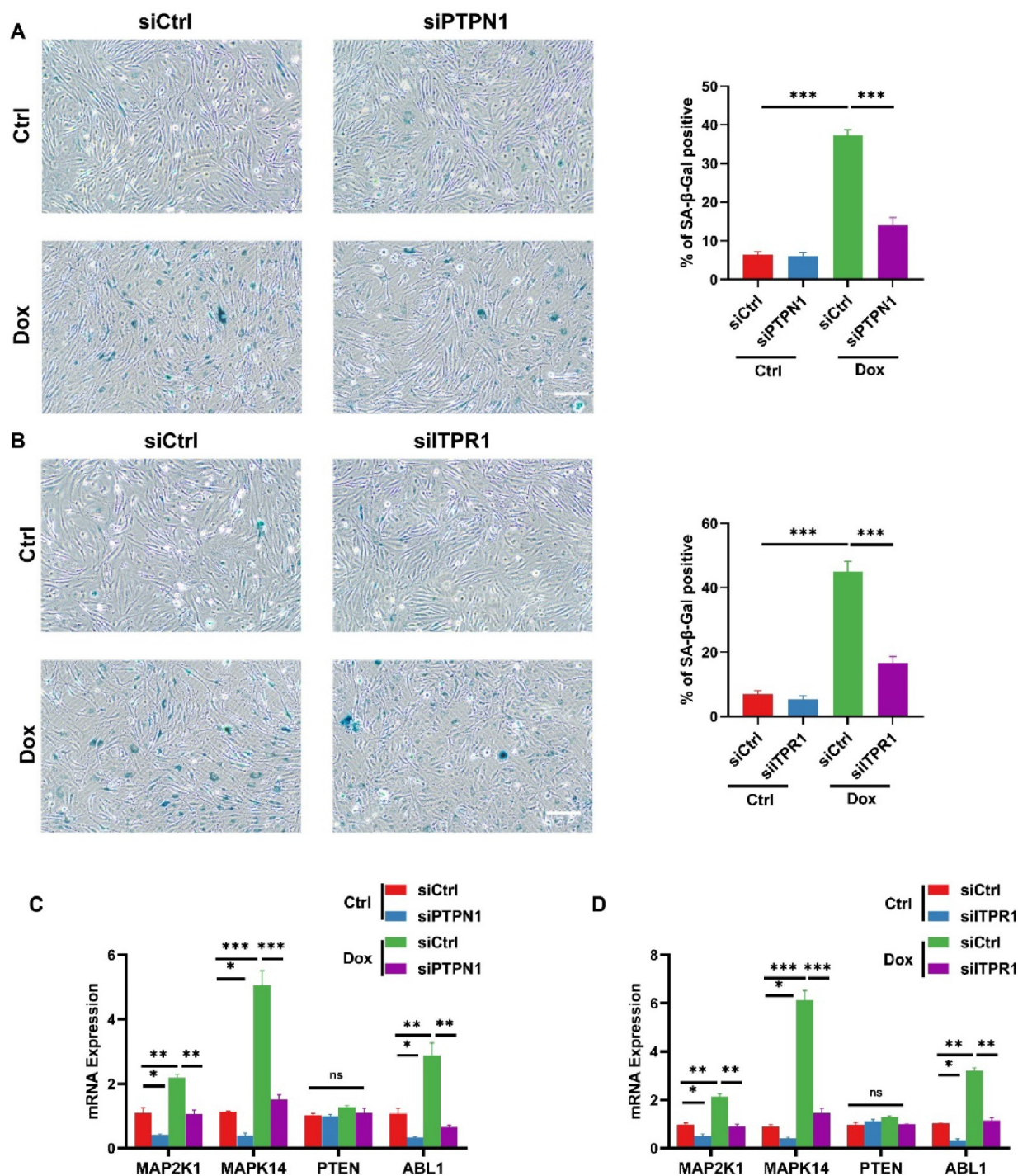


**Figure 9.** (A) Typical pictures of C28/I2 cells stained with SA- $\beta$ -Gal from the control and dox groups treated with or without siRNA targeting PTPN1 (si PTPN1), followed by quantification of C28/I2 cells stained with SA- $\beta$ -Gal.  $n = 3$ , scale bar, 200  $\mu\text{m}$ . (B) Typical pictures of C28/I2 cells stained with SA- $\beta$ -Gal from the control and dox groups treated with or without siRNA targeting ITPR1 (si ITPR1), followed by quantification of the C28/I2 cells stained with SA- $\beta$ -Gal.  $n = 3$ , scale bar, 200  $\mu\text{m}$ . (C) qPCR analysis of mRNA levels of CS-OARGs, including MAP2K1, MAPK14, PTEN, and ABL1 in C28/I2 cells derived from control and dox group treated with or without siPTPN1,  $n = 3$ . (D) qPCR analysis of mRNA levels of CS-OARGs, including MAP2K1, MAPK14, PTEN, and ABL1 in C28/I2 cells derived from control and dox group treated with or without siITPR1,  $n = 3$ , ns  $p > 0.05$ , \* $p < 0.05$ , \*\* $p < 0.01$ , \*\*\* $p < 0.001$ . All data were presented as mean  $\pm$  SEM. One-way analysis of variance with Dunnett's multiple comparisons was used for statistical analysis.

The majority of MAM-OARGs and hub CS-OARGs had a strong association. For instance, the favorably related ITPR1-PTEN combination, which has not yet been fully studied, deserves our entire attention moving ahead. We also found that the expression of MAM-OARGs, such as PTPN1 and ITPR1,

and CS-OARGs, such as PTEN, ABL1, MAPK14, and MAP2K1, was higher expressed in senescent chondrocytes than in the control group by *in vitro* experimental validation. Additionally, the findings of the correlation analysis demonstrated a positive association between MAM-OARGs, including

PTPN1, ITPR1, and CS-OARGs, including PTEN, ABL1, MAPK14, and MAP2K1. Furthermore, this work found that the expression of the CS-OARGs, such as ABL1, MAPK14, and MAP2K1, may be suppressed by PTP1B and ITPR1 knock-down. Therefore, we should focus all of our future efforts on figuring out how exactly PTPN1 and ITPR1 control MAM formation and their influence on cellular senescence in the pathomechanism of OA.

There are still certain limitations, despite the fact that this study made extensive use of bioinformatic techniques to collect a wealth of valuable data that were then verified by trials. First, while we attempted to elucidate whether MAM-related genes may be associated with genes related to cellular senescence in OA, the current study's analysis was very superficial, necessitating more investigation. Second, no more study has been done on the process of gene expression; it will be the focus of future studies. Gene expression has been studied only using bioinformatic techniques and *in vitro* tests. Finally, no *in vivo* tests were carried out to confirm the function.

## CONCLUSIONS

In this study, hub MAM-OARGs were shown to have a strong correlation with genes relevant to cellular senescence in OA. Results of *in vitro* experiments further demonstrated a positive correlation between MAM-OARGs (PTPN1 and ITPR1) and cellular senescence-related and OA-related genes (PTEN, ABL1, MAPK14, and MAP2K1). As a result, our findings can offer new insights into the investigations of MAM-related genes and cellular senescence-related genes, which could be linked to the OA as well as brand-new potential treatment targets.

## ASSOCIATED CONTENT

### Data Availability Statement

Original data are available from corresponding authors: zjewwei@zju.edu.cn and tengchong1984@zju.edu.cn. This paper does not report the original code. Any additional information required to reanalyze the data reported in this paper is available from the lead contact upon request. The links of the GEO data sets used in the present study were listed as follows: 1. GSE207881: <https://www.ncbi.nlm.nih.gov/geo/query/acc.cgi?acc=GSE207881>.

## AUTHOR INFORMATION

### Corresponding Authors

**Chong Teng** – Department of Orthopedics, The Fourth Affiliated Hospital of School of Medicine, and International School of Medicine, International Institutes of Medicine, Zhejiang University, Yiwu, Zhejiang 322000, PR China; [orcid.org/0009-0008-7850-669X](https://orcid.org/0009-0008-7850-669X);

Email: [tengchong1984@zju.edu.cn](mailto:tengchong1984@zju.edu.cn)

**Wei Wei** – Department of Orthopedics, The Fourth Affiliated Hospital of School of Medicine, and International School of Medicine, International Institutes of Medicine, Zhejiang University, Yiwu, Zhejiang 322000, PR China; [orcid.org/0000-0002-2234-4459](https://orcid.org/0000-0002-2234-4459); Email: [zjewwei@zju.edu.cn](mailto:zjewwei@zju.edu.cn)

### Authors

**Hui-Min Li** – Department of Orthopedics, The Fourth Affiliated Hospital of School of Medicine, and International School of Medicine, International Institutes of Medicine, Zhejiang University, Yiwu, Zhejiang 322000, PR China; [orcid.org/0000-0002-6846-2610](https://orcid.org/0000-0002-6846-2610)

**Chenhuan Wang** – Department of Orthopedics, The Fourth Affiliated Hospital of School of Medicine, and International School of Medicine, International Institutes of Medicine, Zhejiang University, Yiwu, Zhejiang 322000, PR China

**Qixue Liu** – Department of Orthopedics, The Fourth Affiliated Hospital of School of Medicine, and International School of Medicine, International Institutes of Medicine, Zhejiang University, Yiwu, Zhejiang 322000, PR China

**Zhicheng Tong** – Department of Orthopedics, The Fourth Affiliated Hospital of School of Medicine, and International School of Medicine, International Institutes of Medicine, Zhejiang University, Yiwu, Zhejiang 322000, PR China

**Binghua Song** – Department of Orthopedics, The Fourth Affiliated Hospital of School of Medicine, and International School of Medicine, International Institutes of Medicine, Zhejiang University, Yiwu, Zhejiang 322000, PR China

Complete contact information is available at:

<https://pubs.acs.org/10.1021/acsomega.3c10316>

## Author Contributions

<sup>†</sup>H.-M.L and C.W contributed equally to the work and should be regarded as cofirst authors. H.-M.L., W.W., and C.T. designed the study. C.H.W., Q.X.L., and Z.C.T. performed the experiments. H.-M.L., C.H.W., Q.X.L., and Z.C.T. performed the statistical analysis. H.-M.L., W.W., and C.T. drafted the article. H.-M.L., B.H.S., W.W., and C.T. supervised the experimental work. All authors contributed to the article and approved the submitted version.

## Notes

The authors declare no competing financial interest.

## ABBREVIATIONS

OA, osteoarthritis; MAMRGs, mitochondria-associated endoplasmic reticulum membrane-related genes; GEO, Gene Expression Omnibus; CS-OARGs, cellular senescence-related and OA-related genes; GO, gene ontology

## REFERENCES

- (1) Loeser, R. F.; Goldring, S. R.; Scanzello, C. R.; Goldring, M. B. Osteoarthritis: a disease of the joint as an organ. *Arthritis Rheumatol.* **2012**, *64* (6), 1697–1707.
- (2) Hootman, J. M.; Helmick, C. G. Projections of US prevalence of arthritis and associated activity limitations. *Arthritis Rheumatol.* **2006**, *54* (1), 226–229.
- (3) Hunter, D. J.; Bierma-Zeinstra, S. Osteoarthritis. *Lancet* **2019**, *393* (10182), 1745–1759.
- (4) Zhao, B.; Zhang, Q.; He, Y.; Cao, W.; Song, W.; Liang, X. Targeted metabolomics reveals the aberrant energy status in diabetic peripheral neuropathy and the neuroprotective mechanism of traditional Chinese medicine JinMaiTong. *J. Pharm. Anal.* **2024**, *14* (2), 225–243.
- (5) Liang, X.-L.; Ouyang, L.; Yu, N.-N.; Sun, Z.-H.; Gui, Z.-K.; Niu, Y.-L.; He, Q.-Y.; Zhang, J.; Wang, Y. Histone deacetylase inhibitor pracinostat suppresses colorectal cancer by inducing CDK5-Drp1 signaling-mediated peripheral mitofission. *J. Pharm. Anal.* **2023**, *13* (10), 1168–1182.
- (6) Fan, R.; Cai, L.; Liu, H.; Chen, H.; Chen, C.; Guo, G.; Xu, J. Enhancing metformin-induced tumor metabolism destruction by glucose oxidase for triple-combination therapy. *J. Pharm. Anal.* **2024**, *14* (3), 321–334.
- (7) Martel-Pelletier, J.; Barr, A. J.; Cicuttini, F. M.; Conaghan, P. G.; Cooper, C.; Goldring, M. B.; Goldring, S. R.; Jones, G.; Teichtahl, A. J.; Pelletier, J. P. Osteoarthritis. *Nat. Rev. Dis. Primers* **2016**, *2*, 16072.
- (8) Prieto-Alhambra, D.; Judge, A.; Javadi, M. K.; Cooper, C.; Diez-Perez, A.; Arden, N. K. Incidence and risk factors for clinically

diagnosed knee, hip and hand osteoarthritis: Influences of age, gender and osteoarthritis affecting other joints. *Ann. Rheum. Dis.* **2014**, *73* (9), 1659–1664.

(9) Chen, Q.-L.; Chen, X.-Y.; Zhu, L.; Chen, H.-B.; Ho, H.-M.; Yeung, W.-P.; Zhao, Z.-Z.; Yi, T. Review on *Saussurea laniceps*, a potent medicinal plant known as “snow lotus”: Botany, phytochemistry and bioactivities. *Phytochem. Rev.* **2016**, *15* (4), 537–565.

(10) Chen, Q. L.; Zhu, L.; Tang, Y. N.; Kwan, H. Y.; Zhao, Z. Z.; Chen, H. B.; Yi, T. Comparative evaluation of chemical profiles of three representative ‘snow lotus’ herbs by UPLC-DAD-QTOF-MS combined with principal component and hierarchical cluster analyses. *Drug Test. Anal.* **2017**, *9* (8), 1105–1115.

(11) Chen, Q.; Zhu, L.; Yip, K. M.; Tang, Y.; Liu, Y.; Jiang, T.; Zhang, J.; Zhao, Z.; Yi, T.; Chen, H. A hybrid platform featuring nanomagnetic ligand fishing for discovering COX-2 selective inhibitors from aerial part of *Saussurea laniceps* Hand.-Mazz. *J. Ethnopharmacol.* **2021**, *271*, 113849.

(12) Li, H. M.; Liu, Y.; Zhang, R. J.; Ding, J. Y.; Shen, C. L. Vitamin D receptor gene polymorphisms and osteoarthritis: A meta-analysis. *Rheumatology* **2021**, *60* (2), 538–548.

(13) Roach, H. I.; Yamada, N.; Cheung, K. S.; Tilley, S.; Clarke, N. M.; Oreffo, R. O.; Kokubun, S.; Bronner, F. Association between the abnormal expression of matrix-degrading enzymes by human osteoarthritic chondrocytes and demethylation of specific CpG sites in the promoter regions. *Arthritis Rheumatol.* **2005**, *52* (10), 3110–3124.

(14) Ziegler, D. V.; Vindrieux, D.; Goehrig, D.; Jaber, S.; Collin, G.; Griveau, A.; Wiel, C.; Bendridi, N.; Djebali, S.; Farfariello, V.; et al. Calcium channel ITPR2 and mitochondria–ER contacts promote cellular senescence and aging. *Nat. Commun.* **2021**, *12* (1), 720.

(15) Wieckowski, M. R.; Giorgi, C.; Lebedzinska, M.; Duszynski, J.; Pinton, P. Isolation of mitochondria-associated membranes and mitochondria from animal tissues and cells. *Nat. Protoc.* **2009**, *4* (11), 1582–1590.

(16) Herrera-Cruz, M. S.; Simmen, T. Of yeast, mice and men: MAMs come in two flavors. *Biol. Direct* **2017**, *12* (1), 3.

(17) Lu, Y.; Luo, Q.; Jia, X.; Tam, J. P.; Yang, H.; Shen, Y.; Li, X. Multidisciplinary strategies to enhance therapeutic effects of flavonoids from *Epimedium Folium*: Integration of herbal medicine, enzyme engineering, and nanotechnology. *J. Pharm. Anal.* **2023**, *13* (3), 239–254.

(18) Park, C. S.; Kang, M.; Kim, A.; Moon, C.; Kim, M.; Kim, J.; Yang, S.; Jang, L.; Jang, J. Y.; Kim, H. H. Fragmentation stability and retention time-shift obtained by LC-MS/MS to distinguish sialylated N-glycan linkage isomers in therapeutic glycoproteins. *J. Pharm. Anal.* **2023**, *13* (3), 305–314.

(19) Han, X.; Ning, Y.; Dou, X.; Wang, Y.; Shan, Q.; Shi, K.; Wang, Z.; Ding, C.; Hao, M.; Wang, K.; et al. *Cornus officinalis* with high pressure wine steaming enhanced anti-hepatic fibrosis: Possible through SIRT3-AMPK axis. *J. Pharm. Anal.* **2023**.

(20) Perrone, M.; Caroccia, N.; Genovese, I.; Missiroli, S.; Modesti, L.; Pedriali, G.; Vezzani, B.; Vitto, V. A. M.; Antenori, M.; Lebedzinska-Arciszewska, M.; et al. The role of mitochondria-associated membranes in cellular homeostasis and diseases. *Int. Rev. Cell Mol. Biol.* **2020**, *350*, 119–196.

(21) Ziegler, D. V.; Martin, N.; Bernard, D. Cellular senescence links mitochondria-ER contacts and aging. *Commun. Biol.* **2021**, *4* (1), 1323.

(22) Li, H. M.; Liu, Y.; Ding, J. Y.; Zhang, R.; Liu, X. Y.; Shen, C. L. In silico Analysis Excavates A Novel Competing Endogenous RNA Subnetwork in Adolescent Idiopathic Scoliosis. *Front. Med.* **2020**, *7*, 583243.

(23) Tong, Z.; Li, H.; Jin, Y.; Sheng, L.; Ying, M.; Liu, Q.; Wang, C.; Teng, C. Mechanisms of ferroptosis with immune infiltration and inflammatory response in rotator cuff injury. *Genomics* **2023**, *115* (4), 110645.

(24) Kulshov, M. V.; Jones, M. R.; Rouillard, A. D.; Fernandez, N. F.; Duan, Q.; Wang, Z.; Koplev, S.; Jenkins, S. L.; Jagodnik, K. M.; Lachmann, A.; et al. Enrichr: A comprehensive gene set enrichment analysis web server 2016 update. *Nucleic Acids Res.* **2016**, *44* (W1), W90–W97.

(25) Szklarczyk, D.; Morris, J. H.; Cook, H.; Kuhn, M.; Wyder, S.; Simonovic, M.; Santos, A.; Doncheva, N. T.; Roth, A.; Bork, P.; et al. The STRING database in 2017: Quality-controlled protein-protein association networks, made broadly accessible. *Nucleic Acids Res.* **2017**, *45* (D1), D362–D368.

(26) Goldring, M. B.; Birkhead, J. R.; Suen, L. F.; Yamin, R.; Mizuno, S.; Glowacki, J.; Arbisser, J. L.; Apperley, J. F. Interleukin-1 beta-modulated gene expression in immortalized human chondrocytes. *J. Clin. Invest.* **1994**, *94* (6), 2307–2316.

(27) Janikiewicz, J.; Szymanski, J.; Malinska, D.; Patalas-Krawczyk, P.; Michalska, B.; Duszynski, J.; Giorgi, C.; Bonora, M.; Dobrzyn, A.; Wieckowski, M. R. Mitochondria-associated membranes in aging and senescence: Structure, function, and dynamics. *Cell Death Dis.* **2018**, *9* (3), 332.

(28) Moltedo, O.; Remondelli, P.; Amodio, G. The Mitochondria–Endoplasmic Reticulum Contacts and their Critical Role in Aging and Age-Associated Diseases. *Front. Cell Dev. Biol.* **2019**, *7*, 172.

(29) Petkovic, M.; O’Brien, C. E.; Jan, Y. N. Interorganelle communication, aging, and neurodegeneration. *Genes Dev.* **2021**, *35* (7–8), 449–469.

(30) Area-Gomez, E.; Del Carmen Lara Castillo, M.; Tambini, M. D.; Guardia-Laguarta, C.; de Groof, A. J.; Madra, M.; Ikenouchi, J.; Umeda, M.; Bird, T. D.; Sturley, S. L.; et al. Upregulated function of mitochondria-associated ER membranes in Alzheimer disease. *EMBO J.* **2012**, *31* (21), 4106–4123.

(31) Filadi, R.; Penden, D.; Pizzo, P. Mitofusin 2: From functions to disease. *Cell Death Dis.* **2018**, *9* (3), 330.

(32) Burkewitz, K.; Feng, G.; Dutta, S.; Kelley, C. A.; Steinbaugh, M.; Cram, E. J.; Mair, W. B. Atf-6 Regulates Lifespan through ER-Mitochondrial Calcium Homeostasis. *Cell Rep.* **2020**, *32* (10), 108125.

(33) Lee, K. S.; Huh, S.; Lee, S.; Wu, Z.; Kim, A. K.; Kang, H. Y.; Lu, B. Altered ER–mitochondria contact impacts mitochondria calcium homeostasis and contributes to neurodegeneration in vivo in disease models. *Proc. Natl. Acad. Sci. U. S. A.* **2018**, *115* (38), No. E8844–E8853.

(34) Gomez-Suaga, P.; Bravo-San Pedro, J. M.; Gonzalez-Polo, R. A.; Fuentes, J. M.; Niso-Santano, M. ER–mitochondria signaling in Parkinson’s disease. *Cell Death Dis.* **2018**, *9* (3), 337.

(35) Denton, R. M. Regulation of mitochondrial dehydrogenases by calcium ions. *Biochim. Biophys. Acta* **2009**, *1787* (11), 1309–1316.

(36) Bell, C. J.; Bright, N. A.; Rutter, G. A.; Griffiths, E. J. ATP regulation in adult rat cardiomyocytes: time-resolved decoding of rapid mitochondrial calcium spiking imaged with targeted photoproteins. *J. Biol. Chem.* **2006**, *281* (38), 28058–28067.

(37) Wiel, C.; Lallet-Daher, H.; Gitenay, D.; Gras, B.; Le Calve, B.; Augert, A.; Ferrand, M.; Prevarskaya, N.; Simonnet, H.; Vindrieux, D.; et al. Endoplasmic reticulum calcium release through ITPR2 channels leads to mitochondrial calcium accumulation and senescence. *Nat. Commun.* **2014**, *5*, 3792.

(38) Yang, M.; Haase, A. D.; Huang, F. K.; Coulis, G.; Rivera, K. D.; Dickinson, B. C.; Chang, C. J.; Pappin, D. J.; Neubert, T. A.; Hannon, G. J.; et al. Dephosphorylation of tyrosine 393 in argonaute 2 by protein tyrosine phosphatase 1B regulates gene silencing in oncogenic RAS-induced senescence. *Mol. Cell* **2014**, *55* (5), 782–790.

(39) Gagarina, V.; Gabay, O.; Dvir-Ginzberg, M.; Lee, E. J.; Brady, J. K.; Quon, M. J.; Hall, D. J. SirT1 enhances survival of human osteoarthritic chondrocytes by repressing protein tyrosine phosphatase 1B and activating the insulin-like growth factor receptor pathway. *Arthritis Rheumatol.* **2010**, *62* (5), 1383–1392.

(40) Bobrich, M. A.; Schwabe, S. A.; Brobeil, A.; Viard, M.; Kamm, M.; Mooren, F. C.; Kruger, K.; Tag, C.; Wimmer, M. PTPIP51: A new interaction partner of the insulin receptor and PKA in adipose tissue. *J. Obes.* **2013**, *2013*, 476240.

(41) Stoica, R.; De Vos, K. J.; Paillusson, S.; Mueller, S.; Sancho, R. M.; Lau, K. F.; Vizcay-Barrena, G.; Lin, W. L.; Xu, Y. F.; Lewis, J.; et al. ER-mitochondria associations are regulated by the VAPB-PTPIP51 interaction and are disrupted by ALS/FTD-associated TDP-43. *Nat. Commun.* **2014**, *5*, 3996.

(42) Del Rey, M. J.; Valin, A.; Usategui, A.; Ergueta, S.; Martin, E.; Municio, C.; Canete, J. D.; Blanco, F. J.; Criado, G.; Pablos, J. L. Senescent synovial fibroblasts accumulate prematurely in rheumatoid arthritis tissues and display an enhanced inflammatory phenotype. *Immun. Ageing* **2019**, *16* (1), 29.

(43) Diekman, B. O.; Sessions, G. A.; Collins, J. A.; Knecht, A. K.; Strum, S. L.; Mitin, N. K.; Carlson, C. S.; Loeser, R. F.; Sharpless, N. E. Expression of p16(INK)(4a) is a biomarker of chondrocyte aging but does not cause osteoarthritis. *Aging Cell* **2018**, *17* (4), No. e12771.

(44) Loeser, R. F. Aging and osteoarthritis: the role of chondrocyte senescence and aging changes in the cartilage matrix. *Osteoarthritis Cartilage* **2009**, *17* (8), 971–979.

(45) Zhu, J.; Yang, S.; Qi, Y.; Gong, Z.; Zhang, H.; Liang, K.; Shen, P.; Huang, Y. Y.; Zhang, Z.; Ye, W.; Yue, L.; Fan, S.; Shen, S.; Mikos, A. G.; Wang, X.; Fang, X. Stem cell-homing hydrogel-based miR-29b-5p delivery promotes cartilage regeneration by suppressing senescence in an osteoarthritis rat model. *Sci. Adv.* **2022**, *8* (13), No. eabk0011.